25. T. Naish *et al.*, *Nature* **458**, 322–328 (2009).
26. R. McKay *et al.*, *Proc. Natl. Acad. Sci. U.S.A.* **109**, 6423–6428 (2012).
27. A. N. LeGrande, G. A. Schmidt, *Geophys. Res. Lett.* **33**, L12604 (2006).
28. A. H. Orsi, G. C. Johnson, J. L. Bullister, *Prog. Oceanogr.* **43**, 55–109 (1999).
29. Z. Zhang, K. H. Nisancioglu, U. S. Ninnemann, *Nat. Commun.* **4**, 1499 (2013).
30. M. E. Raymo, B. Grant, M. Horowitz, G. H. Rau, *Mar. Micropaleontol.* **27**, 313–326 (1996).
31. A. C. Ravelo, D. H. Andreasen, *Geophys. Res. Lett.* **27**, 1001–1004 (2000).
32. J. D. Wright, K. G. Miller, *Paleoceanography* **11**, 157–170 (1996).
33. C.-D. Hillenbrand, D. K. Fütterer, "Neogene to Quaternary deposition of opal on the continental rise west of the Antarctic Peninsula, ODP leg 178, sites 1095, 1096, and 1101," *Proceedings of the Ocean Drilling Program, Scientific Results*, P. F. Barker, A. Camerlenghi, G. D. Acton, A. T. S. Ramsay, Eds. (Ocean Drilling Program, College Station, TX, 2001), vol. 178, pp. 1–33.
34. D. M. Sigman, S. L. Jaccard, G. H. Haug, *Nature* **428**, 59–63 (2004).
35. D. A. Hodell, K. A. Venz-Curtis, *Geochem. Geophys. Geosyst.* **7**, Q09001 (2006).
36. A. Martínez-Garcia *et al.*, *Nature* **476**, 312–315 (2011).
37. L. Menviel, A. Timmermann, O. E. Timm, A. Mouchet, *Paleoceanography* **25**, PA4231 (2010).
38. N. J. Shackleton, J. Imbrie, M. A. Hall, *Earth Planet. Sci. Lett.* **65**, 233–244 (1983).

ACKNOWLEDGMENTS

We thank N. Venti and K. Billups for providing samples and J. Crisicone, N. Abdul, and R. Mortlock for lab assistance. Funding was provided by NSF grants EAR-1052257 and OCE-1334691. B.K.C. thanks Rutgers Aresty Undergraduate Research Fellowship for its support.

SUPPLEMENTARY MATERIALS

www.sciencemag.org/content/346/6211/847/suppl/DC1
Materials and Methods
Supplementary Text
Figs. S1 to S8
References (*39*–*84*)

5 May 2014; accepted 10 October 2014
Published online 23 October 2014;
10.1126/science.1255586

CLIMATE CHANGE

Projected increase in lightning strikes in the United States due to global warming

David M. Romps,[1]* Jacob T. Seeley,[1] David Vollaro,[2] John Molinari[2]

Lightning plays an important role in atmospheric chemistry and in the initiation of wildfires, but the impact of global warming on lightning rates is poorly constrained. Here we propose that the lightning flash rate is proportional to the convective available potential energy (CAPE) times the precipitation rate. Using observations, the product of CAPE and precipitation explains 77% of the variance in the time series of total cloud-to-ground lightning flashes over the contiguous United States (CONUS). Storms convert CAPE times precipitated water mass to discharged lightning energy with an efficiency of 1%. When this proxy is applied to 11 climate models, CONUS lightning strikes are predicted to increase 12 ± 5% per degree Celsius of global warming and about 50% over this century.

Lightning exerts a powerful control on atmospheric chemistry through its generation of nitrogen oxides, especially in the middle and upper troposphere (*1*–*3*). As the primary trigger for wildfires, lightning also shapes the evolution of species and ecosystems (*4*, *5*). Despite its importance, the future increase in lightning flash rates due to global warming remains poorly constrained: Estimates range from 5% (*6*, *7*) to over 100% (*8*) per degree Celsius (°C) of global mean temperature increase. Here we show that a simple proxy—the product of the convective instability and the precipitation rate—explains most of the variance in lightning flashes over the contiguous United States (CONUS). When applied to global climate models (GCMs), this proxy predicts a mean increase in flash rate of 12% per global-mean °C over the CONUS. This augurs significant changes in the future atmospheric chemistry and wildfire frequency of North America.

Previous estimates of the sensitivity of lightning flash rates to global mean temperature have relied on ad hoc proxies for use in GCMs or observed correlations between temperature and lightning (or lighting proxies). One GCM parameterization sets the total flash rate (in flashes per minute) equal to a constant times the maximum cloud height to the fifth power (*9*), and later

[1]Department of Earth and Planetary Science, University of California, Berkeley, and Earth Sciences Division, Lawrence Berkeley National Laboratory, Berkeley, CA, USA.
[2]Department of Atmospheric and Environmental Sciences, State University of New York at Albany, Albany, NY, USA.
*Corresponding author. E-mail: romps@berkeley.edu

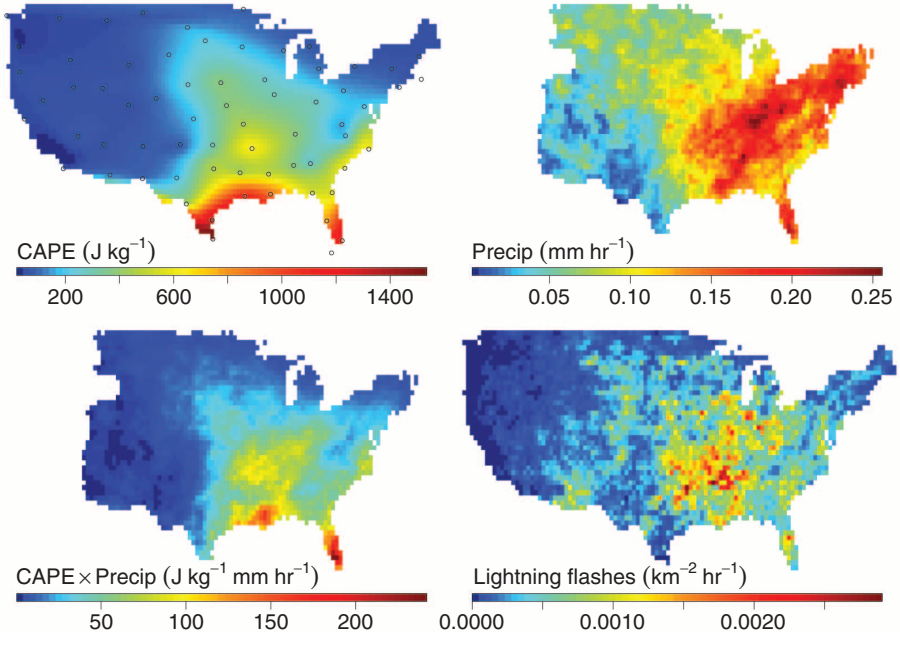

Fig. 1. Mean maps of CAPE, precipitation, CAPE times precipitation, and lightning flashes. For the year 2011, maps are shown of mean (**top left**) CAPE from the SPARC radiosonde data, (**top right**) precipitation from the National Weather Service River Forecast Center data, (**bottom left**) product of the top two maps, and (**bottom right**) CG lightning from the NLDN data. For CAPE, means are calculated by averaging all 00 and 12 GMT soundings; circles denote the locations of radiosonde releases. For precipitation and lightning, means are calculated by averaging over 22-02 and 10-14 GMT.

papers extended this to cloud-to-ground (CG) lightning [e.g., (*10*)]. Despite this proxy's lack of dependence on area (making it sensitive to GCM grid spacing) or on the amount of storm activity (making it insensitive to the rain rate), it is the most widely used proxy for lightning (*6*, *7*, *11*, *12*), generating estimates for the increase in global flash rate ranging from 5% per °C to 16% per °C. Observational estimates also predict a wide range, but at much higher values. At some specific weather stations, flash rates increase with wet-bulb temperature over the seasonal cycle at rates in the range of 100 to 800% per °C (*13*). A similar analysis using satellite lightning data gives interannual sensitivities for Northern Hemisphere land and the globe of 56% per °C and 40% per °C, respectively (*14*). Using the fundamental mode of the Schumann resonance as a proxy for flash rate, a global sensitivity of 100% per °C is found (*8*). Although these estimates have the advantage of being rooted in observations, it is unlikely that these intraseasonal and interseasonal relationships are the same as those in a global warming scenario. By developing a new proxy for lightning that is physically motivated, testable with observations, and applicable to GCMs, a more robust projection is sought here for the CONUS, which is a major contributor to global lightning (*15*).

Here we propose that the lightning flash rate per area is proportional to the precipitation rate times convective available potential energy (CAPE). This proxy combines the observed linearity of flash rate on precipitation rate (*16*–*19*) with suggestions that flashes are positively correlated with CAPE (*20*–*23*). In mathematical form,

$$F = \frac{\eta}{E} \times P \times \mathrm{CAPE} \qquad (1)$$

where F is the lightning flash rate per area ($m^{-2}\ s^{-1}$), P is the precipitation rate ($kg\ m^{-2}\ s^{-1}$), and CAPE is in $J\ kg^{-1}$. Using an adiabatic definition of CAPE, the product of CAPE and P is the theoretical maximum rate at which kinetic energy is imparted to ascending water condensates, in units of $W\ m^{-2}$. The constant of proportionality, η/E, contains the dimensionless conversion efficiency η and the energy discharge per flash E (in joules). The efficiency η is the ratio of power per area dissipated by lightning to the CAPE per area per time available to condensates. We do not propose here a specific charging mechanism, but we note that most charging mechanisms are consistent with the notion that higher updraft speeds and water contents should yield higher flash rates.

In this study, we focused on the CONUS because it is well instrumented. Three sets of data were used, which overlap during the year 2011. CAPE is calculated from SPARC (Stratosphere-troposphere Processes And their Role in Climate) radiosonde data (*24*), P is taken from the National Oceanic and Atmospheric Administration River Forecast Centers (*25*), and CG lightning flashes are obtained from the National Lightning Detection Network [NLDN (*26*, *27*)]; for more details, see the supplementary materials. The means of these quantities during 2011 are shown in Fig. 1.

Also shown in Fig. 1 is the pointwise product of the annual mean CAPE map and the annual mean P map. This map of CAPE × P (lower left panel) bears a close resemblance to the map of lightning flashes (lower right panel). In particular, both CAPE × P and the flash rate maximize in Florida and in the states adjacent to the Mississippi and Ohio rivers. This distribution of flashes is similar to the long-term annual mean [see Fig. 1 of (*28*)], because we are sampling lightning in the local morning and evening, which correspond to the trough and peak of the CONUS mean diurnal cycle [see Fig. 2 of (*28*)].

To assess the performance of the CAPE × P proxy, we focus here on the time series of CONUS

Table 1. Future changes predicted by GCMs. Predicted changes in global mean temperature (ΔT) and percent per global mean °C changes in CONUS annual mean CAPE (ΔCAPE), precipitation (ΔPr), and CG lightning flash rate (ΔCG) are shown for 11 CMIP5 GCMs. Changes are calculated for the years 2079–2088 of the RCP8.5 experiment relative to the years 1996–2005 of the historical experiment.

GCM	ΔT (°C)	ΔCAPE (%°C)	ΔPr (%°C)	ΔCG (%°C)
BCC-CSM1.1	3.4	6.4	-0.6	3.4
BCC-CSM1.1(m)	3.1	8.8	-0.2	6.9
CanESM2	4.7	12.9	4.2	17.3
CCSM4	3.9	7.3	2.0	9.1
CNRM-CM5	3.9	9.9	2.6	12.2
FGOALS-g2	3.1	11.5	-1.8	7.0
GFDL-CM3	5.0	16.5	2.6	17.6
GFDL-ESM2M	2.5	13.4	2.7	15.9
MIROC5	3.4	15.1	0.3	16.3
MRI-CGCM3	3.4	12.5	3.0	14.7
NorESM1-M	3.6	8.5	1.4	10.3
Mean:	3.6	11.2	1.5	11.9

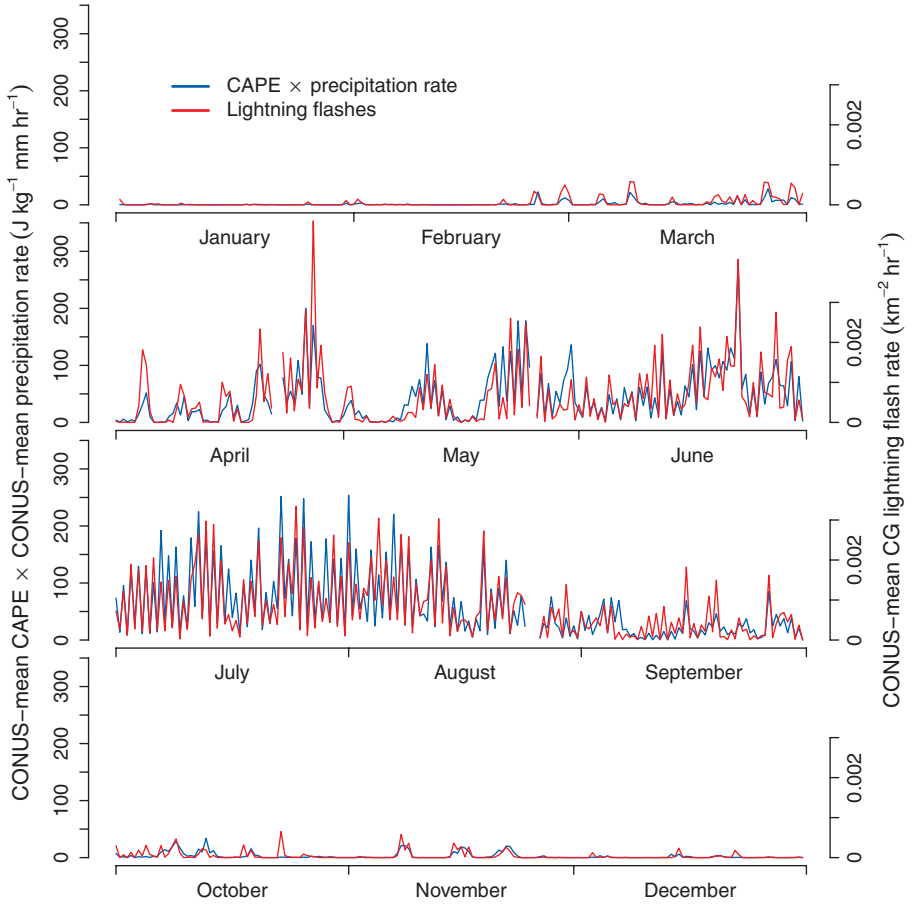

Fig. 2. Time series of the proxy and observed lightning flashes. For the year 2011, time series are shown of 0 and 12 GMT (blue) CONUS mean precipitation times CONUS mean CAPE and (red) CONUS mean CG lightning flash rate.

mean CAPE, precipitation, and lightning. A spatially resolved evaluation of Eq. 1 is not attempted here because of practical difficulties stemming from the sparsity of CAPE measurements and the fact that convection releases CAPE. The latter fact precludes using the product of colocated precipitation and CAPE; instead, a CAPE value nearby, but upwind, of a storm should be used. With the sparse network of noisy CAPE measurements, this is a challenging task that is left to future work.

Figure 2 plots two time series for the entire year of 2011: the product of CONUS mean CAPE and CONUS mean precipitation rate in blue (axes on the left), and CONUS mean CG lightning flash rate in red (axes on the right). The proxy varies in synchrony with the flash rate on a range of time scales, from the diurnal [high at 0 Greenwich mean time (GMT), low at 12 GMT] to the seasonal (high in spring and summer, low in fall and winter) and time scales in between (high during periods of sustained storminess, low in the lulls between). The proxy successfully captures the varying magnitude of the flash rate, as well. In the fall and winter, both the proxy and the flash rate have peak values about one order of magnitude smaller than their peak values in the spring and summer.

The lower right panel of Fig. 3 shows the scatter plot of the CAPE × P and flash-rate time series. They are related to each other in a linear fashion, and the proxy explains 77% of the variance in the lightning flash rate. This can be compared with other candidates, such as P, the maximum height of convection [level of neutral buoyancy (LNB)] to the fifth power, and CAPE, which explain only 29, 39, and 52% of the variance, respectively. The CAPE × P proxy also explains a substantial amount of the lightning variance within a season: 69% for January, February, March; 65% for April, May, June; 75% for July, August, September; and 40% for October, November, December.

Using the fact that 1 mm of precipitation equals 1 kg m^{-2} of liquid water, the best-fit line in the lower right panel is described by Eq. 1 with $\eta/E = 1.3 \times 10^{-11}$ J^{-1}. A best estimate for the energy released by a midlatitude CG lightning flash is about 1 GJ, although estimates range from a few tenths of a GJ to several GJ (*1*). Using E = 1 GJ, we obtain an efficiency of η = 0.01. In other words, 1% of the CAPE that could be theoretically extracted by water (i.e., CAPE times the processed water mass) is converted to electrical potential energy that is then discharged by CG lightning.

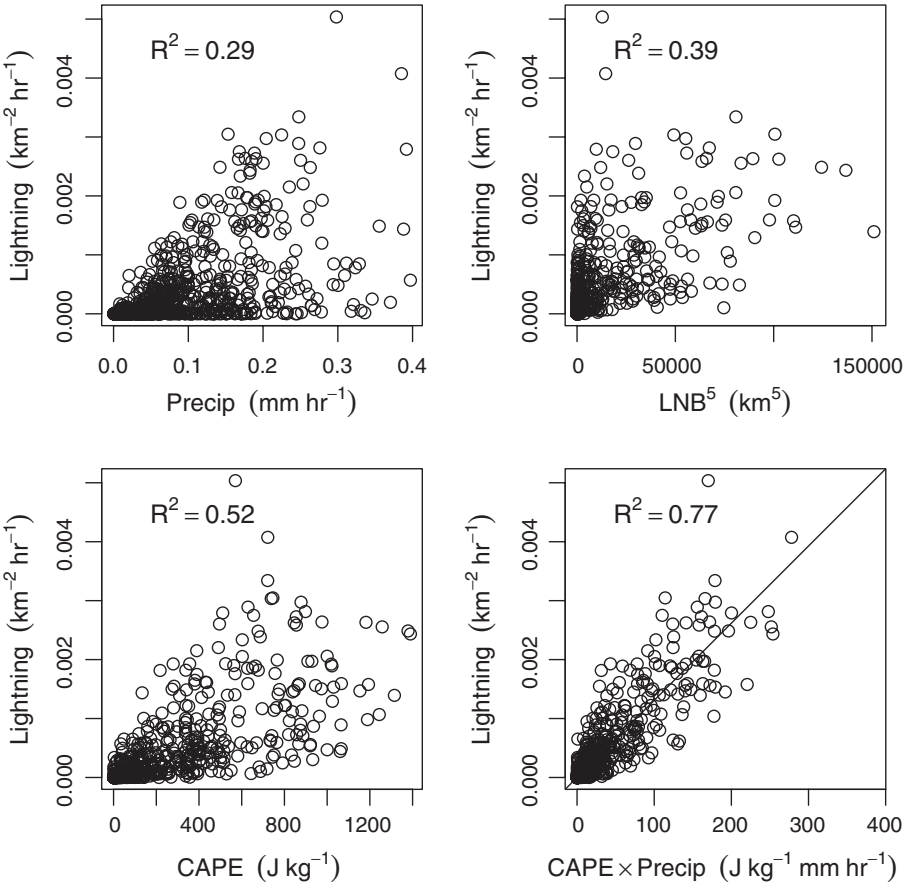

Fig. 3. Lightning versus various proposed proxies. For the year 2011, scatter plots are shown of the time series of 0 and 12 GMT CONUS mean lightning against **(top left)** precipitation, **(top right)** LNB to the fifth power, **(bottom left)** CAPE, and **(bottom right)** CAPE times precipitation.

Given the success of CAPE × P in replicating the time series of observed lightning flashes, it is a natural candidate for assessing future changes in flash rates due to global warming. Previous studies of GCM simulations have found that global warming causes CAPE to increase over much of Earth (*29*, *30*) and over the CONUS in particular (*31*–*33*). Similar results have been found in much simpler cloud-resolving simulations, in which CAPE increases with sea surface temperature (*34*–*36*). Recent work has provided insight into why this increase in CAPE occurs (*36*). In addition, the global precipitation rate is expected to increase with global temperature (*37*), although the predicted changes in annual mean precipitation are of variable sign across the United States.

To assess how these future changes will affect lightning, we analyzed output from 11 GCMs in the Coupled Model Intercomparison Project Phase 5 [CMIP5 (*38*)]; see the supplementary materials for more details. Table 1 lists the CONUS mean fractional changes in CAPE and precipitation for the GCMs in our ensemble. To account for differences in climate sensitivity between the models, we report these results as percent changes per °C of global warming. All GCMs in our ensemble predict that CONUS mean CAPE will increase over the 21st century, with a mean increase of 11.2% per °C of global warming. There is a high level of agreement between the models on the spatial pattern and magnitude of this CAPE increase (fig. S1). On the other hand, there is significantly more variation in the GCMs' predictions for future precipitation; the mean response is a 1.5% increase per °C of global warming, but some models predict decreased precipitation over the CONUS.

The percent change in annual mean lightning flash rate can be estimated as the mean percent change in the product of CAPE and precipitation time series between the years 1996–2005 and 2079–2088. Using this method, all GCMs in our ensemble predict annual mean lightning-strike frequency in the United States to increase, with a mean increase of 12% per °C (column 5 of Table 1). The standard deviation of the ensemble's predictions is 5% per °C; therefore, we can conclude that the rate of CG lightning strikes over the CONUS is likely to increase as a function of global mean temperature at a rate of 12 ± 5% per °C. Overall, the GCMs predict a ~50% increase in the rate of lightning strikes in the CONUS over the 21st century.

REFERENCES AND NOTES

1. U. Schumann, H. Huntrieser, *Atmos. Chem. Phys.* **7**, 3823–3907 (2007).
2. H. Levy II, W. J. Moxim, P. S. Kasibhatla, *J. Geophys. Res.* **101**, 22911 (1996).
3. V. Grewe, *Sci. Total Environ.* **374**, 167–181 (2007).
4. W. J. Bond, J. E. Keeley, *Trends Ecol. Evol.* **20**, 387–394 (2005).
5. J. G. Pausas, J. E. Keeley, *Bioscience* **59**, 593–601 (2009).
6. C. Price, D. Rind, *J. Geophys. Res.* **99**, 10823 (1994).
7. N. Michalon, A. Nassif, T. Saouri, J. F. Royer, C. A. Pontikis, *Geophys. Res. Lett.* **26**, 3097–3100 (1999).
8. E. R. Williams, *Science* **256**, 1184–1187 (1992).
9. C. Price, D. Rind, *J. Geophys. Res.* **97**, 9919–9933 (1992).

10. C. Price, D. Rind, *Mon. Weather Rev.* **122**, 1930–1939 (1994).
11. A. Banerjee *et al.*, *Atmos. Chem. Phys.* **14**, 9871–9881 (2014).
12. A. Krause, S. Kloster, S. Wilkenskjeld, H. Paeth, *J. Geophys. Res.: Biogeosci.* **119**, 312 (2014).
13. E. R. Williams, *Mon. Weather Rev.* **122**, 1917–1929 (1994).
14. N. Reeve, R. Toumi, *Q. J. R. Meteorol. Soc.* **125**, 893–903 (1999).
15. H. J. Christian *et al.*, *J. Geophys. Res.* **108**, 4005 (2003).
16. L. J. Battan, *J. Atmos. Sci.* **22**, 79–84 (1965).
17. A. Tapia, J. A. Smith, M. Dixon, *J. Appl. Meteorol.* **37**, 1497–1509 (1998).
18. W. A. Petersen, S. A. Rutledge, *J. Geophys. Res.* **103**, 14025 (1998).
19. E. W. Meijer, P. F. J. van Velthoven, D. W. Brunner, H. Huntrieser, H. Kelder, *Phys. Chem. Earth, Part C Sol.-Terr. Planet. Sci.* **26**, 577–583 (2001).
20. E. R. Williams *et al.*, *J. Atmos. Sci.* **49**, 1386–1395 (1992).
21. E. Williams *et al.*, *J. Geophys. Res., D, Atmospheres* **107**, 8082 (2002).
22. S. D. Pawar, D. M. Lal, P. Murugavel, *Atmos. Res.* **106**, 44–49 (2012).
23. P. Murugavel, S. D. Pawar, V. Gopalakrishan, *Int. J. Climatol.* **34**, 3179–3187 (2014).
24. SPARC, U.S. High Vertical Resolution Radiosonde Data, Stratosphere-troposphere Processes and their Role in Climate (2013).
25. D. Kitzmiller, D. Miller, R. Fulton, F. Ding, *J. Hydrol. Eng.* **18**, 133–142 (2013).
26. R. S. Wacker, R. E. Orville, *J. Geophys. Res.* **104**, 2151 (1999).
27. R. E. Orville, G. R. Huffines, *Mon. Weather Rev.* **129**, 1179–1193 (2001).
28. R. L. Holle, *Mon. Weather Rev.* **142**, 1037–1052 (2014).
29. B. Ye, A. D. Del Genio, K. K. W. Lo, *J. Clim.* **11**, 1997–2015 (1998).
30. A. H. Sobel, S. J. Camargo, *J. Clim.* **24**, 473–487 (2011).
31. R. J. Trapp *et al.*, *Proc. Natl. Acad. Sci. U.S.A.* **104**, 19719–19723 (2007).
32. R. J. Trapp, N. S. Diffenbaugh, A. Gluhovsky, *Geophys. Res. Lett.* **36**, L01703 (2009).
33. N. S. Diffenbaugh, M. Scherer, R. J. Trapp, *Proc. Natl. Acad. Sci. U.S.A.* **110**, 16361–16366 (2013).
34. D. M. Romps, *J. Atmos. Sci.* **68**, 123–138 (2011).
35. C. J. Muller, P. A. O'Gorman, L. E. Back, *J. Clim.* **24**, 2784–2800 (2011).
36. M. S. Singh, P. A. O'Gorman, *Geophys. Res. Lett.* **40**, 4398–4403 (2013).
37. I. M. Held, B. J. Soden, *J. Clim.* **19**, 5686–5699 (2006).
38. K. E. Taylor, R. J. Stouffer, G. A. Meehl, *Bull. Am. Meteorol. Soc.* **93**, 485–498 (2012).

ACKNOWLEDGMENTS

D.M.R. acknowledges support from the Scientific Discovery through Advanced Computing (SciDAC) program funded by the U.S. Department of Energy Office of Advanced Scientific Computing Research and Office of Biological and Environmental Research, and by the U.S. Department of Energy's Earth System Modeling, an Office of Science, Office of Biological and Environmental Research program under contract no. DE-AC02-05CH11231. J.T.S. acknowledges support from the National Science Foundation (NSF) Graduate Research Fellowship under grant no. DGE1106400. D.V. and J.M. acknowledge support from NSF under grant no. AGS1132576. Thanks are due to the SPARC data center for archiving the high-resolution radiosonde data and making them publicly available. The authors are also grateful to J. Paul, B. Lawrence, K. Sugioka, and N. Jeevanjee for their help with the precipitation data. Thanks also to three anonymous reviewers. Data sources are described in the online supplementary materials.

SUPPLEMENTARY MATERIALS

www.sciencemag.org/content/346/6211/851/suppl/DC1
Methods
Fig. S1
References

23 July 2014; accepted 20 October 2014
10.1126/science.1259100

CIRCADIAN RHYTHM

Dysrhythmia in the suprachiasmatic nucleus inhibits memory processing

Fabian Fernandez,[2] Derek Lu,[1] Phong Ha,[1] Patricia Costacurta,[1] Renee Chavez,[1] H. Craig Heller,[1] Norman F. Ruby[1]*

Chronic circadian dysfunction impairs declarative memory in humans but has little effect in common rodent models of arrhythmia caused by clock gene knockouts or surgical ablation of the suprachiasmatic nucleus (SCN). An important problem overlooked in these translational models is that human dysrhythmia occurs while SCN circuitry is genetically and neurologically intact. Siberian hamsters (*Phodopus sungorus*) are particularly well suited for translational studies because they can be made arrhythmic by a one-time photic treatment that severely impairs spatial and recognition memory. We found that once animals are made arrhythmic, subsequent SCN ablation completely rescues memory processing. These data suggest that the inhibitory effects of a malfunctioning SCN on cognition require preservation of circuitry between the SCN and downstream targets that are lost when these connections are severed.

Deficits in cognitive performance caused by disrupted circadian timing have become a growing concern among health care professionals (*1*). Recent clinical studies have found that age-related declines in circadian function can lead to mild cognitive impairment or dementia (*2*, *3*). These memory deficits are not simply a consequence of poorer sleep, because reductions in circadian rhythm amplitude and robustness can accelerate progression of mild cognitive impairment or dementia even when sleep quality is maintained (*2*, *3*). The observation that circadian timing is substantially weakened among people with Alzheimer's disease has raised the possibility that cognitive deficits might be treated by improving circadian function (*4*–*6*). However, there are no mouse or rat models of adult-onset circadian dysfunction in genetically and neurologically intact animals living in standard laboratory conditions.

Rodent models of chronic circadian arrhythmia such as clock gene knockouts or surgical ablation of the central circadian pacemaker, the suprachiasmatic nucleus (SCN), exhibit no or only modest deficits in declarative memory. Clock gene knockouts of *cryptochrome 1 and 2* or *period 1 and 2* are arrhythmic, and they exhibit normal spontaneous alternation behavior, long-term spatial memory for food rewards, and contextual memory for environments associated with foot shock (*7*, *8*), although *cryptochrome 1 and 2* knockouts do fail to learn time-place associations (*7*). *Bmal1* knockouts are also arrhythmic and exhibit normal contextual fear conditioning and novel object recognition; however, they navigate poorly in the Morris water maze (*9*). In the instances where knockout mice exhibit performance deficits, it is unclear whether memory impairments are due to arrhythmia, to pleiotropic gene effects, or to abnormalities during brain development (*10*). Mice and rats with SCN lesions exhibit no substantial impairment in avoidance tasks, recognition memory, spatial learning, or reversal spatial learning but have modest deficits in contextual fear conditioning and in the water maze probe test (*11*–*14*). In some studies, SCN ablation actually improves task performance (*11*, *12*).

The marginal effect of clock gene knockouts and SCN lesions on memory stands in stark contrast to the well-documented adverse effects of shift work and jet lag on cognition (*15*). One critical factor that often gets overlooked in relating animal circadian studies to human conditions is the fact that human dysrhythmia occurs while the SCN circuitry remains intact both genetically and structurally. We evaluated the possibility that intact SCN circuitry is necessary for circadian dysfunction to interfere with memory processing by using the Siberian hamster (*Phodopus sungorus*) model of circadian arrhythmia. This model has been used to study homeostatic sleep mechanisms, where its value compared to clock gene knockout and SCN lesion models of arrhythmia has been recognized (*16*).

Siberian hamsters exhibit phase-resetting responses to single light pulses that are typical of nocturnal rodents (Fig. 1A), yet their response to two light signals is quite different. When these animals are given a phase-advancing light signal on one night, followed by a phase-delaying light signal on the next night, circadian timing is completely abolished within a few days, even though each signal given alone does not disrupt their circadian organization (Fig. 1B). This disruptive phase shift (DPS) protocol causes arrhythmia by suppressing the amplitude of clock gene oscillations within the SCN to zero, thereby driving the clock to its singularity point (*17*, *18*). Induction of arrhythmia at the genetic and behavioral levels occurs within a few days and lasts indefinitely despite the continued presence of a daily light-dark cycle (*18*, *19*).

The DPS protocol allowed us to evaluate recognition and spatial memory in arrhythmic Siberian

[1]Biology Department, Stanford University, Stanford CA, USA. [2]Department of Psychiatry and Behavioral Sciences, Stanford University, Palo Alto, CA, USA.
*Corresponding author. E-mail: ruby@stanford.edu